JOC Article

Analysis of Conformational Equilibria in Aplidine Using Selective Excitation 2D NMR Spectroscopy and Molecular Mechanics/Dynamics Calculations

Francisco Cárdenas,[†] Josep Maria Caba,[‡] Miguel Feliz,[†] Paul Lloyd-Williams,*[,§] and Ernest Giralt*[,‡,§]

Unitat de RMN d'Alt Camp, Universitat de Barcelona, Josep Samitier 1, E-08028 Barcelona, Spain, Department of Organic Chemistry, University of Barcelona, Martí i Franquès, 1-11, Barcelona E-08028, Spain, and Institut de Recerca Biomèdica de Barcelona, Parc Científic de Barcelona, Josep Samitier 1, E-08028 Barcelona, Spain

lloyd@qo.ub.es; egiralt@qo.ub.es

Received June 10, 2003

Aplidine (dehydrodidemnin B), a natural product with potent antitumor activity currently in multicenter phase II clinical trials, exists in DMSO as a mixture of four slowly interconverting conformations in a ratio of 47:33:13:7. NMR spectroscopy shows that these arise as a consequence of *cis*/*trans* isomerization about the NMe-Leu^7-Pro^8 and Pro^8-Pyr amide bonds of the molecule's side chain. Two major conformations account for 47% and 33% of the total population, a ratio of 60:40 between the two. They correspond to the *cis*- and *trans*-isomers, respectively, about the Pro^8-Pyr amide bond. Two minor conformers arise as a consequence of similar isomerism about the Pro^8-Pyr amide bond, but in structures in which the NMe-Leu^7-Pro^8 amide bond is *cis* rather than *trans*. These account for approximately 13% and 7% of the total population, corresponding to a ratio of 65:35 *cis*/*trans*, respectively. Molecular dynamics simulations show that the three-dimensional structures of all four conformational isomers are similar in the macrocycle and that all are essentially unchanged with respect to the macrocycle of didemnin B. Significant differences in the conformation of the molecule's side chain are, however, observed between major and minor pairs. Analysis of hydrogen-bonding patterns shows that each major conformer exhibits a β-turn like structure and is stabilized by hydrogen bonding between a different carbonyl group of the pyruvyl unit of the molecule's side chain and the NH of the Thr^6 residue. The minor isomers have a *cis*-amide bond between the NMe-Leu^7 and Pro^8 residues that obliges the side chain to adopt an extended disposition where hydrogen bonding to the macrocycle is absent. These results suggest that the ability of the molecule's side chain to adopt a β-turn-like conformation may not be a prerequisite for biological activity in the didemnins and that conformations having an extended side-chain may play a role in the biological activity of aplidine.

Introduction

Interest in the didemnin family of marine depsipeptides[1−3] stretches back over more than 20 years, since they were first isolated and characterized by Rinehart in 1981. Structurally these molecules consist of a 23-membered macrocycle, common to all members of the family, which has a pendant side chain whose makeup differentiates the various didemnins. Certain members of the family exhibit very promising biological activity, in particular a marked ability to inhibit cell proliferation, which has stimulated much effort into their development for therapeutic use.[4−8] A recent extensive review by one of the major contributors to the field[9] provides an overview of chemical, structural, and biological studies on the didemins to date.

One of the key unresolved issues is that of the detailed mode of action.[9] Previous work has demonstrated that even subtle changes in structure can profoundly affect biological activity. An illustration of this is provided by didemnin B and aplidine (dehydrodidemnin B, DDB). The

* Corresponding author.
[†] Unitat de RMN d'Alt Camp, Universitat de Barcelona.
[‡] Institut de Recerca Biomèdica de Barcelona.
[§] Department of Organic Chemistry, University of Barcelona.

(1) Li, W.-R.; Joullié, M. M. In *Studies in Natural Products*; Atta-ur-Rahman, Ed.; Elsevier Science Publishers: New York, 1992; Vol. 10, Part F, p 241.
(2) Sakai, R.; Rinehart, K. L.; Kishore, V.; Kundu, B.; Faircloth, G.; Gloer, J. B.; Carney, J. R.; Namikoshi, M.; Sun, F.; Hughes, R. G.; Gravalos, D. G.; de Quesada, T. G.; Wilson, G. R.; Heid, R. M. *J. Med. Chem.* **1996**, *39*, 2819.
(3) Sakai, R.; Stroh, J. G.; Sullins, D. W.; Rinehart, K. L. *J. Am. Chem. Soc.* **1995**, *117*, 3734.
(4) Mittelman, A.; Chun, H. G.; Puccio, C.; Coombe, N.; Lansen, T.; Ahmed, T. *Invest. New Drugs* **1999**, *17*, 179.
(5) Sparidans, R. W.; Kettenes-van den Bosch, J. J.; van Tellingen, O.; Nuyen, B.; Henrar, R. E. C.; Jimeno, J. M.; Faircloth, G.; Floriano, P.; Rinehart, K. L.; Beijnen, J. H. *J. Chromatogr.* **1999**, *B 729*, 43.
(6) Schmidt, U.; Griesser, H.; Haas, G.; Kroner, M.; Riedel, B.; Schumacher, A.; Sutoris, F.; Haupt, A.; Emling, F. *J. Peptide Res.* **1999**, *54*, 146.
(7) Liang, B.; Vera, M. D.; Joullié, M. M. *J. Org. Chem.* **2000**, *65*, 4762.
(8) Vervoort, H.; Fenical, W.; Epifanio, R. A. *J. Org. Chem.* **2000**, *65*, 782.
(9) Vera, M. D.; Joullie, M. M. *Med. Res. Rev.* **2002**, *22*, 102.

10.1021/jo034798r CCC: $25.00 © 2003 American Chemical Society
Published on Web 11/13/2003

CHART 1

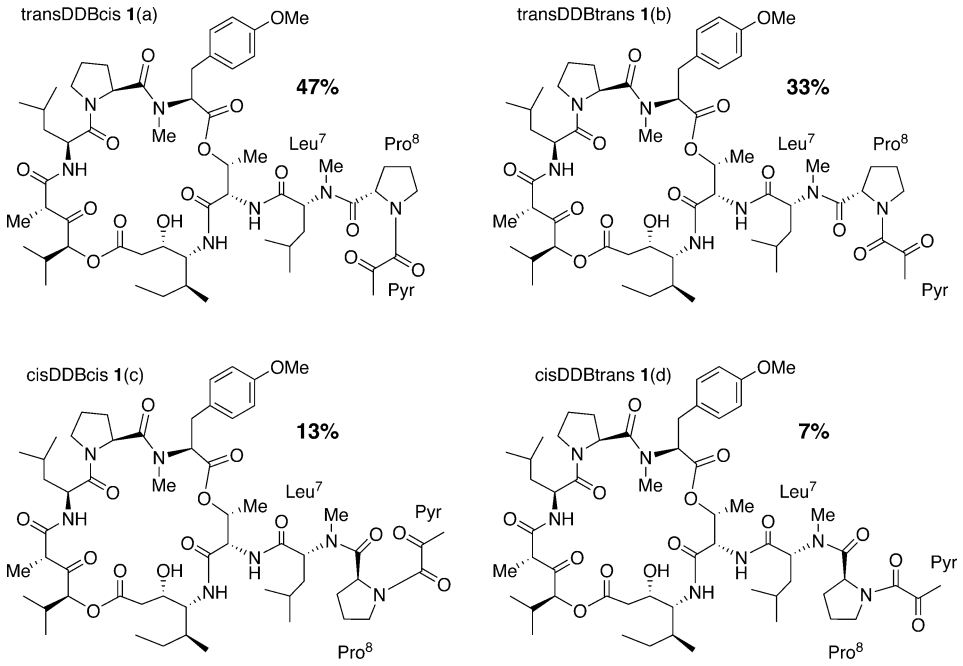

difference between these is merely that the alcohol of the lactyl residue at the side-chain terminus of the former is replaced by its oxidized form, a carbonyl group, in the latter. Such a seemingly trivial structural change, however, leads to an increase of an order of magnitude in the biological activity of aplidine compared to didemnin B. On the other hand, our results, disclosed both here and previously,[10] together with those of other workers,[11−14] indicate that variation in side-chain structure does not result in significant conformational change in the macrocycle. It would seem that, in general, it is the molecule's side chain that is primarily responsible for conformational variation in the didemnins.

The precise role of the side-chain in biological activity is not clear. However, it does appear that, although it is not involved in the union of the depsipeptide with its receptors, it may play an important role in stabilizing the biologically active conformation.[15] There has also been speculation as to whether the ability of the side-chain to adopt a type II β-turn is a requisite for biological activity.[9] In this paper, we attempt to shed further light upon these intriguing issues, and upon the mode of action more generally, through the in-depth study of the conformational behavior of aplidine[5,16−18] in DMSO. This is the most active member of the family presently known and is undergoing multicenter phase II clinical trials.

We have previously[10] reported on the conformational analysis of both natural and synthetic[19] aplidine **1** in $CDCl_3$ and have shown that the molecule exists as 45:55 mixture of two slowly interconverting conformational isomers, **1**(a) and **1**(b) as a consequence of *cis*-/*trans*-isomerism about the terminal Pro^8-Pyr- amide bond.[5,16,17] In our present study, NMR spectroscopy in DMSO-d_6 reveals four distinct interconverting structures in a ratio of 47:33:13:7. Of these, the major conformational isomers are those observed in chloroform, **1**(a) and **1**(b), and are a consequence of the same conformational equilibrium observed in that solvent. The minor ones, **1**(c) and **1**(d), however, arise on account of similar *cis*/*trans* isomerism about the Pro^8-Pyr amide bond, but in structures in which the NMe-Leu^7-Pro^8 amide bond is *cis*. This is the first time that such conformational isomers have been observed in the didemnins (Chart 1).

The results from previous molecular mechanics/dynamics simulations carried out[10] on isomers **1**(a) and **1**(b), together with new studies performed here on all four isomers **1**(a)−**1**(d), provided further information on the three-dimensional structure of aplidine. Analysis of the trajectories indicate that the macrocycles of all four conformational isomers have similar three-dimensional structures to that reported[11,13] for the macrocycle in didemnin B, which exists as one major conformation in solution in both $CHCl_3$ and DMSO. Significant differences are, however, observed between the major and minor pairs of conformers with regard to the disposition of the molecule's side-chain. In the major isomers **1**(a) and **1**(b) this side chain adopts type II β-turn-like conformations, as we have reported previously.[10] In the minor conformers, **1**(c) and **1**(d) however, owing to the presence of the NMe-Leu^7-Pro^8 *cis*-amide bond, it adopts an open, ex-

(10) Cárdenas, F.; Thormann, M.; Feliz, M.; Caba, J.-M.; Lloyd-Williams, P.; Giralt, E. *J. Org. Chem.* **2001**, *66*, 4580.
(11) Kessler, H.; Will, M.; Antel, J.; Beck, H.; Sheldrick, G. M. *Helv. Chim. Acta* **1989**, *72*, 530.
(12) Kessler, H.; Mronga, S.; Will, M.; Schmidt, U. *Helv. Chim. Acta* **1990**, *73*, 25.
(13) Hossain, M. B.; van der Helm, D.; Antel, J.; Sheldrick, G. M.; Sanduja, S. K.; Weinheimer, A. J. *Proc. Natl. Acad. Sci. U.S.A.* **1988**, *85*, 4118.
(14) Hossain, M. B.; van der Helm, D.; Antel, J.; Sheldrick, G. M.; Weinheimer, A. J.; Sanduja, S. K. *Int. J. Peptide Protein Res.* **1996**, *47*, 20.
(15) Shen, G. K.; Zukoski, C. F.; Montgomery, D. W. *Int. J. Immunopharmac.* **1992**, *14*, 63.
(16) Rinehart, K. L. US Patent 5,137,870, 1992.
(17) Rinehart, K. L. US Patent 5,294,603, 1994.
(18) Rinehart, K. L. *Med. Res. Rev.* **2000**, *20*, 1.
(19) Jou, G.; González, I.; Albericio, F.; Lloyd-Williams, P.; Giralt, E. *J. Org. Chem.* **1997**, *62*, 354.

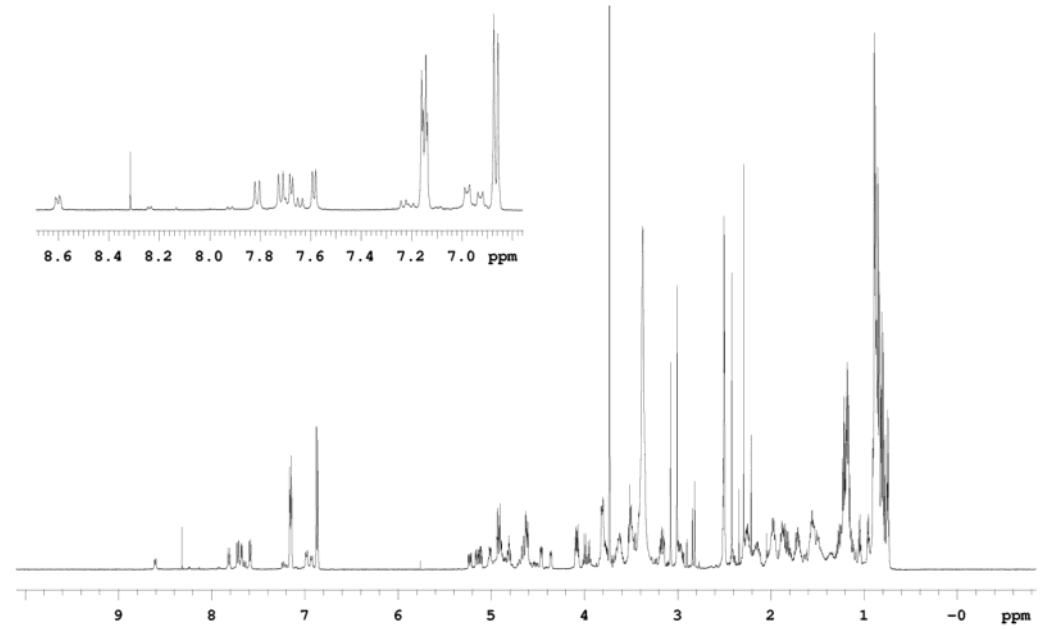

FIGURE 1. ^{1}H NMR spectrum of aplidine in DMSO-d_6, with expanded amide region inset.

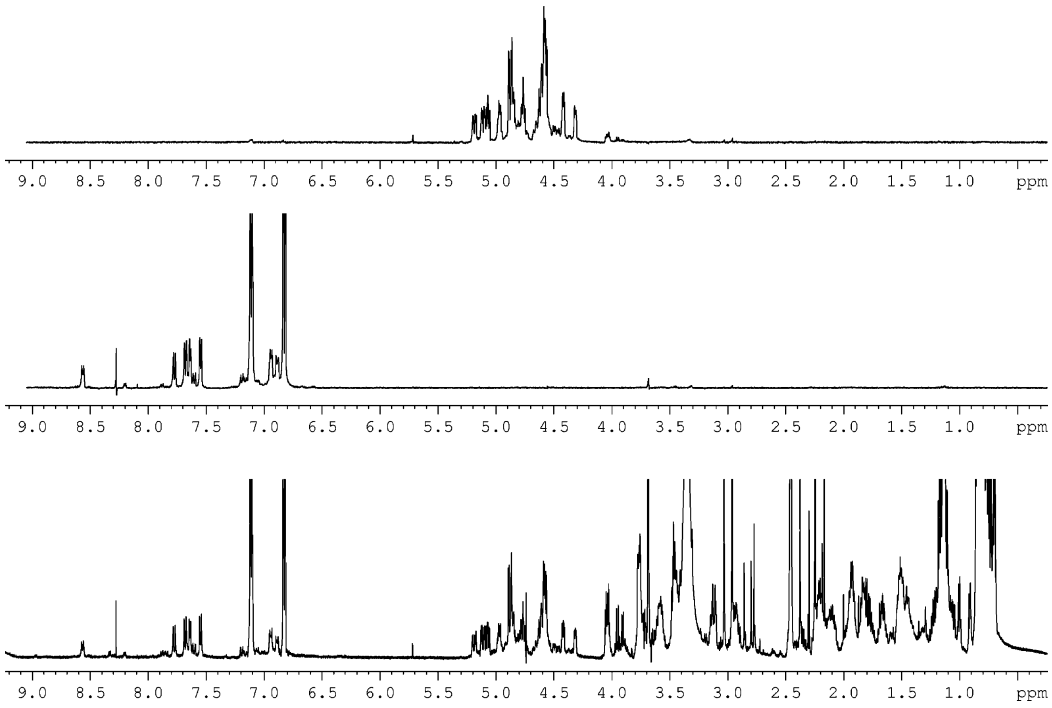

FIGURE 2. Comparison of the complete 500 MHz ^{1}H NMR spectrum of aplidine in DMSO (bottom) with the selective excitation of the amide region (middle spectrum) and of the C_α region (top spectrum).

tended conformation that does not form hydrogen bonds to the macrocycle.

Results and Discussion

NMR Spectroscopy. Aplidine (dehydrodidemnin B) in DMSO gives rise to complex NMR spectra as a consequence of the molecule existing as a mixture of conformational isomers in unequal quantities (Figure 1). This can clearly be seen in the greater than expected complexity of the amide region of the 500 MHz ^{1}H spectrum at 298 K (Figure 2).

The presence of four distinct conformational isomers in relative proportions of 47:33:13:7 was revealed by the integration of the methyl resonances of the terminal pyruvyl residue in the 800 MHz ^{1}H NMR spectrum at 298 K. As in $CDCl_3$, the majority of the macrocycle residues, particularly Ist[1], Pro[4], and Tyr[5], exhibited signal degeneracy.[10] This, together with the unequal distribution of four distinct species within the sample, significantly complicates the assignment of proton and carbon resonances. While homonuclear 3D NMR can increase the resolution of closely spaced signals, its application is

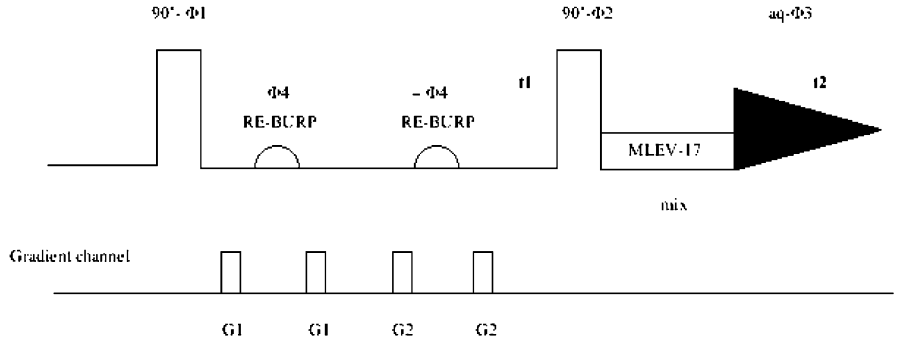

FIGURE 3. Graphical representation of the excitation sculpting pulse sequence corresponding to the ^{1}H NMR-2D-F1-*soft*-TOCSY experiment.

hampered by the long acquisition times and substantial storage capacities required and also by the difficulties associated with data extraction and processing. Since the most relevant structural information is often concentrated in specific regions of a spectrum (e.g., those corresponding to the amide and α-carbon atoms in peptides and proteins) selective excitation of that region through the use of soft pulses during one or more stages of an experiment can provide a less resource-intensive alternative.[20]

Such an approach effectively leads to a reduction in the dimensionality of the NMR experiment so that structural information comparable to that provided by 3D NMR can be obtained from a 2D experiment but with the advantages of increased digital resolution and a reduction in both signal overlap and acquisition times. Recent methods of selective excitation have combined shaped pulse sequences with pulsed field gradients. The double pulsed-field gradient spin−echo (DPFGSE) sequence has allowed the development of the excitation-sculpting method[21] which exhibits a good excitation profile and is useful in the study of complex molecular systems (Figure 3).

The application of 2D-soft-F1-TOCSY and 2D-soft-F1-NOESY experiments using the DPFGSE sequence to the analysis of aplidine in DMSO-d_6, as reported here, allowed all proton resonances of all four isomers to be unambiguously assigned (Figure 4).

The existence of four interconverting species in quite different proportions (47:33:13:7) made the measurement of mid- and long-range NOEs rather challenging, especially in the cases of the minor isomers. As a consequence, we limited ourselves to measuring only those to only those that we were sure could be measured accurately and that provided important structural information. Analysis of these together with $\Delta\delta/\Delta T$ data for the NH resonances of Ist^1 and Leu^3 indicated only relatively minor changes in geometry between the macrocycles of all conformational isomers. (Interproton distances, obtained from a quantitative treatment of the NOE data, are listed in Table S9 in the Supporting Information). The $\Delta\delta/\Delta T$ values observed for the NH resonances of Ist^1 and Leu^3 were less than 1.0 ppb/K, indicating the formation of hydrogen bonds. Taken together these data indicate that the macrocycle in all four conformational

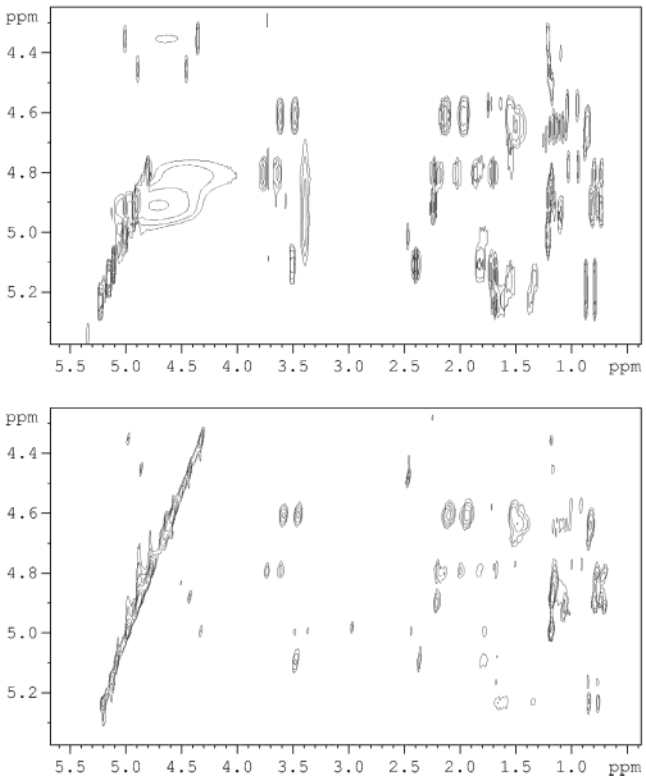

FIGURE 4. Upper spectrum shows a conventional 500 MHz TOCSY spectrum of the C_α region of aplidine in DMSO-d_6 at 298 K, with a digital resolution in F1 and F2 of 2.67 and 21.40 Hz and an acquisition time of 2.4 h. Lower spectrum shows an F1-*soft*-TOCSY spectrum of the same region, with a digital resolution in F1 and F2 of 2.67 and 7.81 Hz and an acquisition time of 1.2 h. The broad peaks at 4.5 and 3.3 ppm peaks in the upper spectrum are artifacts due to non-optimal-phase adjustment for the peak due to water.

isomers adopted the twisted figure of eight conformation previously reported[11−14,22] for didemnin B.

Significant differences between conformers were to be found in the molecule's side-chain, however. Analysis of the chemical shift differences of the β and γ carbon atoms corresponding to the Pro^8 residue as measured in ^{1}H−^{13}C HSQC correlation experiments clearly indicated[23,24]

(20) Roumestand, C.; Delay, C.; Gavin, J. A.; Canet, D. *Magn. Reson. Chem.* **1999**, *37*, 451.
(21) Krishnamurthy, V. V. *Magn. Reson. Chem.* **1997**, *35*, 9.
(22) Searle, M. S.; Hall, J. G.; Kyratzis, I.; Wakelin, L. P. G. *Int. J. Peptide Protein Res.* **1989**, *34*, 445.
(23) Dorman, D. E.; Bovey, F. A. *J. Org. Chem.* **1973**, *38*, 2379.
(24) Kessler, H. *Angew. Chem., Int. Ed. Engl.* **1982**, *21*, 512.

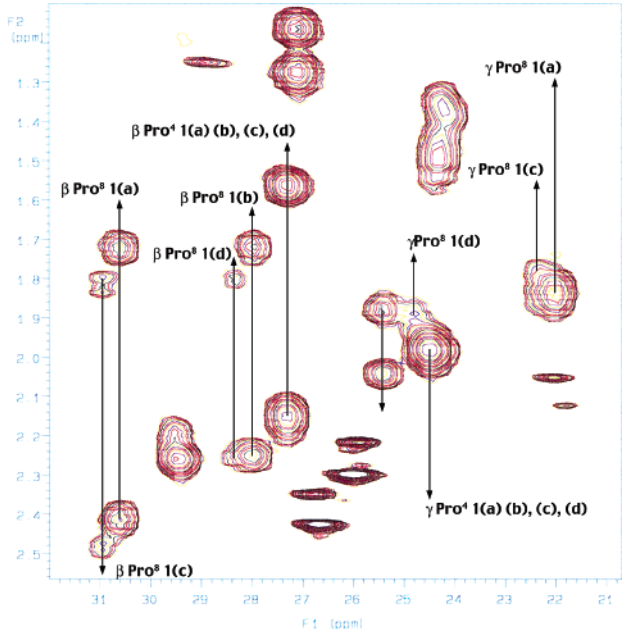

FIGURE 5. Detail of ^{13}C HSQC NMR spectrum showing Pro^4 and Pro^8 β and γ carbons.

cis/*trans*-isomerism about the Pyr-Pro^8 tertiary amide bond, in all four observed conformational isomers. Such a phenomenon has previously been reported for aplidine in $CDCl_3$, which exists as a 45:55 mixture of the slowly interconverting *cis*- and *trans*-isomers of the Pyr-Pro^8 terminal amide bond (Figure 5).

In DMSO-d_6, the same isomers account for 47% and 33%, respectively, of the mixture—a ratio of 60:40 between the two. The *cis*-isomer predominates over the *trans*-isomer in the more polar solvent, as might be expected.[25,26] The key difference between aplidine in $CDCl_3$ and in DMSO-d_6, however, is the presence of two other isomers in the latter solvent in proportions of 13% and 7%, respectively. The detection of a strong NOE between the α-H's of the Leu^7 and Pro^8 residues in both minor conformational isomers clearly indicated that the amide bond between them was in the *cis*-configuration (Figure 6).

Confirmatory evidence was provided by the presence of exchange peaks between the amide protons of isomers **1**(a) and **1**(c) and **1**(b) and **1**(d), respectively, in NOESY experiments at 600 MHz (Figure 7).

The unambiguous detection of an NOE between the α-H's of the NMeLeu^7 and Pro^8 residues in conformational isomer **1**(d), the least abundant of the four and present in an estimated concentration of less than 1.05 mM, in the F1-*soft*-NOESY spectrum at 500 MHz is further testament to the power of the excitation sculpting method. The digital resolution available with this technique is comparable to that of conventional NOESY experiment at 800 MHz, even though there is some concomitant loss of sensitivity as can be appreciated in the NOESY pattern in the 4.8−5.0 ppm region of spectrum (d) (Figure 8).

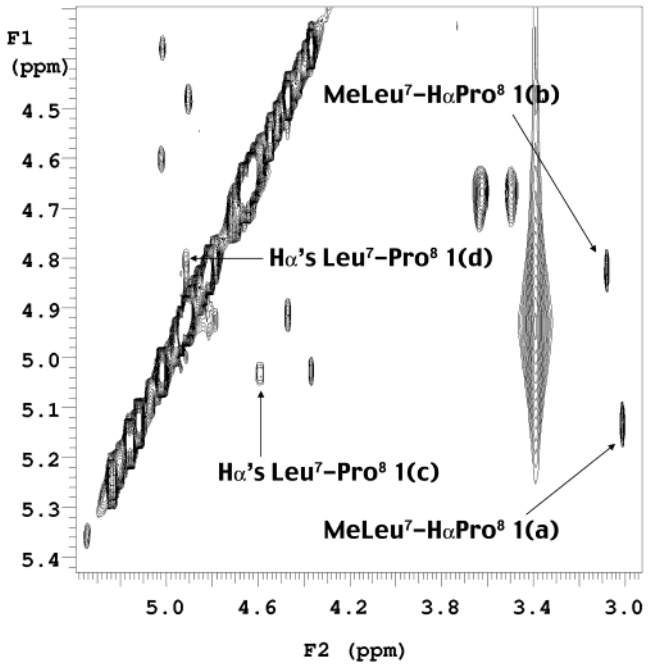

FIGURE 6. Detail of the 600 MHz NOESY spectrum (mixing time 300 ms) of aplidine in DMSO-d_6, showing key NOEs indicating cis/trans isomerism about the NMeLeu^7-Pro^8 tertiary amide bond.

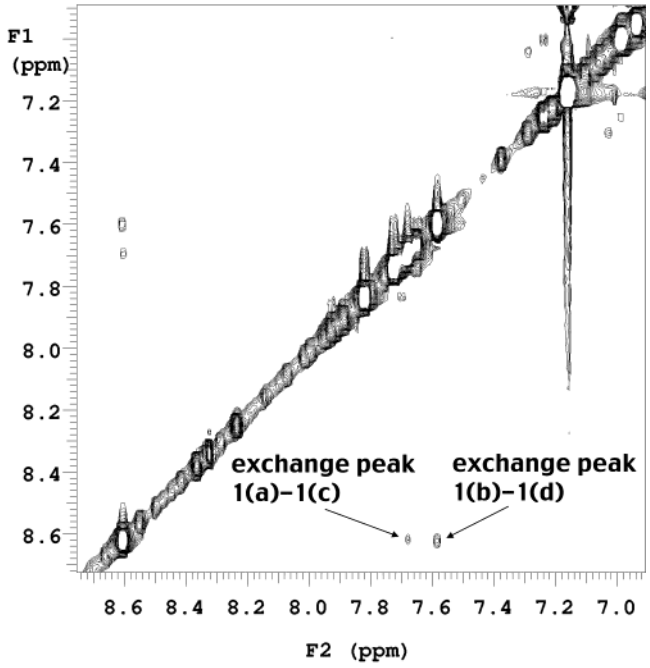

FIGURE 7. Detail of the 600 MHz NOESY spectrum (mixing time 300ms) of aplidine in DMSO-d_6 showing the presence of cross-peaks due to chemical interchange between amide protons.

We estimate a value of $\Delta G^{\ddagger}$ of around 79 kJ mol^{-1} for the free energy of activation for *cis*-/*trans*-isomerization about the Leu^7-Pro^8 amide bond based on the relationship between the integration values for the cross-peaks and the diagonal peaks of the Thr^6 NH resonance in the NOESY spectrum.[27] We previously reported[10] a value of

(25) Ishimoto, B.; Tonan, K.; Ikawa, S.-I. *Spectrochim. Acta, Part A* **1999**, *56A*, 201.
(26) Eberhardt, E. S.; Loh, S. N.; Hinck, A. P.; Raines, R. T. *J. Am. Chem. Soc.* **1992**, *114*, 5437.

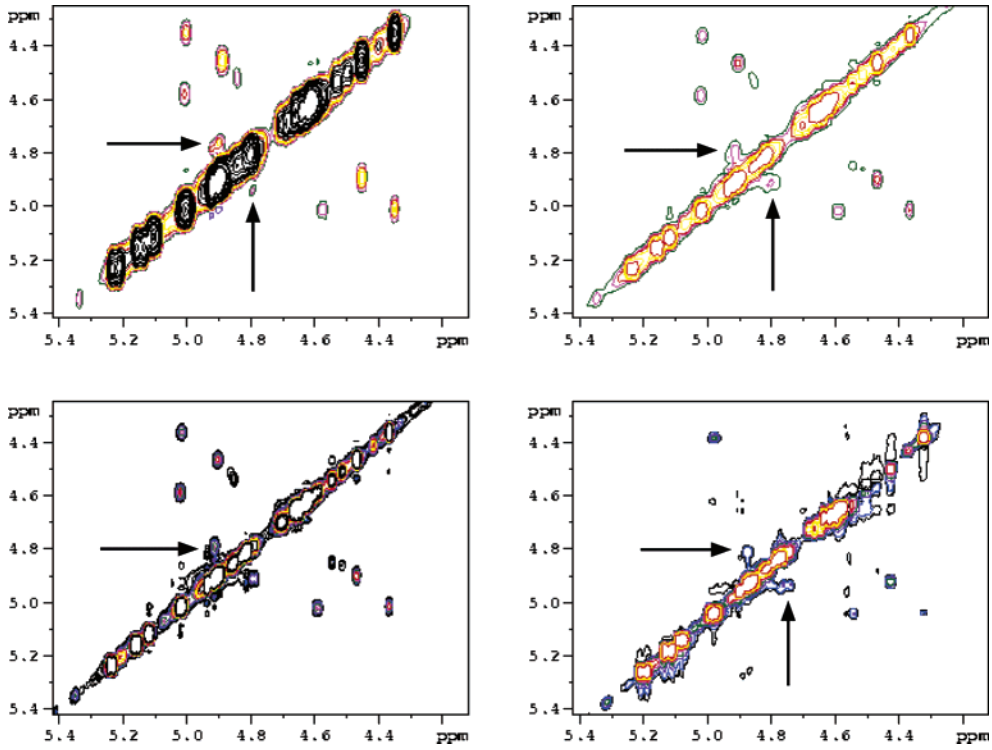

FIGURE 8. Comparison of digital resolutions of (a) conventional NOESY spectrum at 500 MHz, mixing time 300 ms, 2048 × 256 in F1 and F2, 64 scans; (b) conventional NOESY spectrum at 600 MHz, mixing time 300 ms, 2048 × 512 in F1 and F2, 8 scans; (c) conventional NOESY spectrum at 800 MHz, mixing time 300 ms, 3072 × 512 in F1 and F2, 32 scans; (d) F1-*soft*-NOESY spectrum at 500 MHz, mixing time 300 ms, 2048 × 256 in F1 and F2, 128 scans. In each spectrum, the arrows indicate the NOE observed between the H_α's of NMeLeu[7] and Pro[8] of the least abundant conformer **1**(d).

$\Delta G^{\ddagger} = 86.9 \pm 0.8$ kJ mol^{-1} for *cis*-/*trans*-isomerization about the Pro[8]-Pyr amide in DMSO. This latter is between 4 and 8 kJ mol-[1] higher than the value corresponding to a normal[28] peptide tertiary amide bond involving Pro and leads to a rate constant for *cis*-/*trans*-isomerization in DDB of 3.4×10^{-3} s^{-1} at 298K and a value of $t_{1/2}$ of approximately 3.4 min for each isomer.

Molecular Mechanics/Dynamics Calculations. On account of the inherent lack of precision associated with the determination of interproton distances in molecules of the size[29] of aplidine, in addition to the limited number of interatomic distances per residue accessible experimentally, molecular mechanics/dynamics calculations were carried out in order to provide more information on the three-dimensional structures of conformational isomers **1**(a)−**1**(d) of the molecule. Tables of derived quantities (interatomic distances, torsion angles and hydrogen bonding patterns) derived from these calculations, together with results previously obtained[10] for isomers **1**(a) and **1**(b) are collected together in the Supporting Information.

Calculations were performed on each conformational isomer separately using the well-established CHARMm force field[30,31] for reasonably long periods of time (see the Experimental Section) and without distance restraints in order to allow the conformational space of the molecule to be more fully explored. Three implicit descriptions (ϵ = 1, 4.8, and 45) and two explicit solvent models (H_2O and DMSO) were applied.

In all simulations, good agreement between the unrestrained molecular dynamics trajectories in the CHARMM all-atom representation and experimental NMR data from the most informative and clear region of the spectrum was observed and nearly all of the atomic distances that corresponded to the measured NOE distances were within those values that would be expected to produce an NOE. (See Tables S10, S11, S12, and S13 in the Supporting Information.)

Analysis of the most relevant torsion angles found in the simulations (summarized in Tables S14, S15, S16, and S17 in the Supporting Information) provided further evidence for the similarity of the overall three-dimensional structures of the macrocycles of all four conformational isomers. Comparison with reported results for didemnin B by NMR studies[11] and by X-ray diffraction[13] indicated that macrocycle three-dimensional structure was also broadly similar, and in each case adopted a twisted figure of eight conformation.

Analysis of the hydrogen bonds produced in the simulations (see Tables S18, S19, S20 and S21 in the Supporting Information) showed that for all four conformational isomers of DDB the transannular hydrogen bond between Ist[1]-NH and Leu[3]-CO was present in all simulations as was that between Leu[3]-NH and MeLeu[7]-CO. This result is compatible with the low $\Delta\delta/\Delta T$ values in the

(27) Bodenhausen, G.; Ernst, R. R. *J. Am. Chem. Soc.* **1982**, *104*, 1304.
(28) Grathwohl, C.; Wüthrich, K. *Biopolymers* **1981**, *20*, 2623.
(29) Neuhaus, D.; Williamson, M. P. *The Nuclear Overhauser Effect in Structural and Conformational Analysis*, 2nd ed.; John Wiley and Sons: New York, 2000.
(30) Momany, F. A.; Rone, R. *J. Comput. Chem.* **1992**, *13*, 888.
(31) Momany, F. A.; Rone, R.; Kunz, H.; Frey, R. F.; Newton, S. Q.; Schäfer, L. *THEOCHEM* **1993**, *286*, 1.

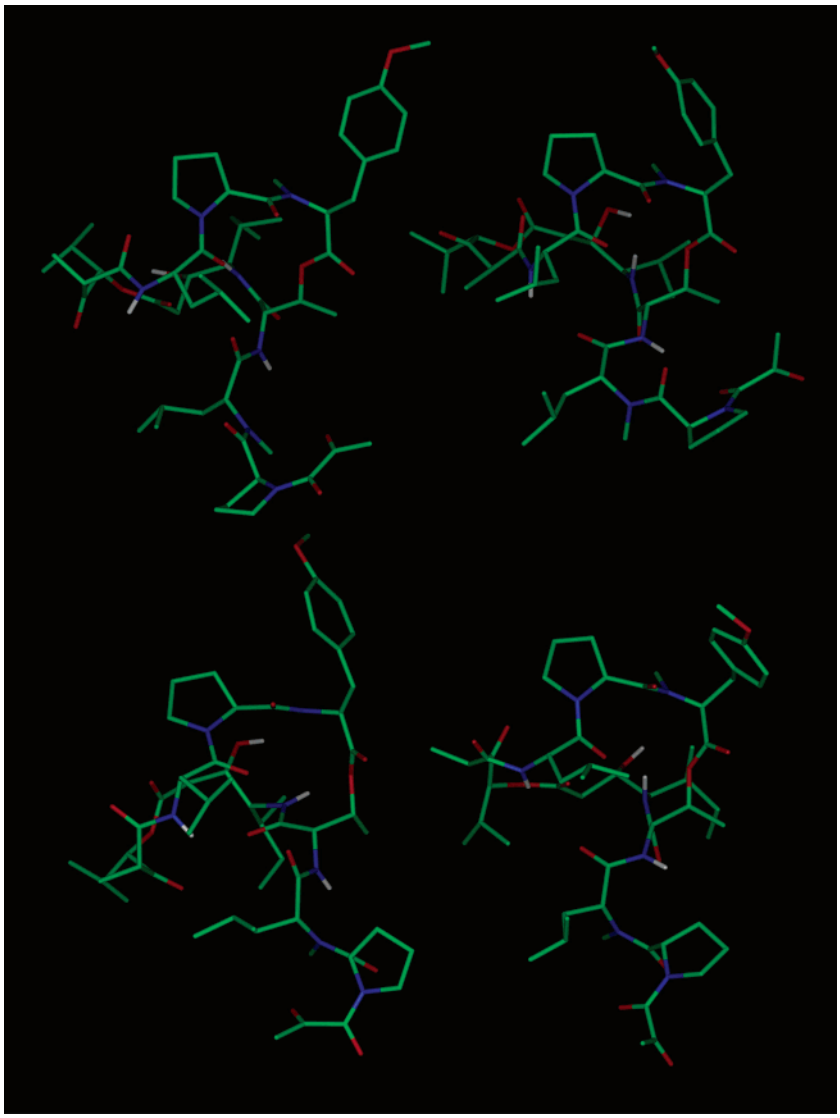

FIGURE 9. Representative snapshots from the explicit DMSO trajectories of (clockwise from top left) *trans*DDB*cis* **1**(a), *trans*DDB*trans* **1**(b), *cis*DDB*trans***1**, (d) and *cis*DDB*cis* **1**(c).

ranges 0.3−1.6 and 1.3−1.6 ppb/K observed by ^{1}H NMR for the Ist^1-NH and Leu^3-NH protons, respectively. Both of these hydrogen bonds have previously been reported in didemnin B and are responsible for the abovementioned figure of eight disposition of the macrocycle. In these simulations, another transannular hydrogen bond between Leu^3-NH and Ist^1-CO was also detected in all simulations except that for the explicit DMSO solvent model in the case of the *trans*DDB*trans* isomer **1**(b).

For both the *trans*DDB*cis* **1**(a) and *trans*DDB*trans* **1**(b) a hydrogen bond between Thr^6-NH and Pro^8-CO was detected in all simulations, except for the explicit DMSO solvent model in the case of isomer **1**(a). However, in the case of *trans*DDB*trans* **1**(b) the hydrogen bond between Thr^6-NH and Pyr-CO^1, analogous to the reported hydrogen bond in didemnin B between Thr^6-NH and Lac-CO, was found in all simulations whereas this hydrogen bond was lacking in all simulations of the *trans*DDB*cis* isomer **1**(a). For the *trans*DDB*cis* isomer **1**(a) on the other hand, a hydrogen bond between Thr^6-NH and Pyr-CO^2 was detected which was not found in any of the simulations of the *trans*DDB*trans* isomer **1**(b).

These data provide an explanation for the predominance of the major conformational isomers of aplidine. The *trans*DDB*trans* isomer **1**(b) is stabilized by the Thr^6-NH to Pyr-CO^1 hydrogen bond in a manner similar to the dominant conformer of didemnin B whereas the *trans*DDB*cis* isomer **1**(a) is stabilized by the hydrogen bond between Thr^6-NH and Pyr-CO^2. These hydrogen bonds appear to stabilize both conformational isomers to a similar degree, consistent with the observed values for $\Delta\delta/\Delta T$ of 3.6 ppb/K for the Thr^6-NH proton in the *cis*- and *trans*-rotamers, respectively. The presence of a weak NOE between the γH of Thr^6 and the methyl group of the pyruvyl unit for both isomers provided further experimental support.

The minor isomers *cis*DDB*cis* **1**(c) and *cis*DDB*trans* **1**(d) show markedly different hydrogen-bonding patterns. The presence of the *cis*-amide bond between the Leu^7 and Pro^8 residues causes the molecule's side-chain to adopt an extended conformation in which no hydrogen bonds between the side chain and the macrocycle were detected in any of the simulations of these two conformers. This lack of hydrogen-bond formation in the side chain of the

molecule is consistent with the values for $\Delta\delta/\Delta T$ of 4.3 ppb/K for the Thr^6-NH proton in the minor *cis*- and *trans*-rotamers.

Representative snapshots of each of the conformational isomers from the explicit DMSO trajectories are shown in Figure 9.

The similarity of the three-dimensional structures of the major conformers **1**(a) and **1**(b) is illustrated by the superposition of representative snapshots of both isomers from the trajectories of the DMSO explicit-solvent simulations as shown in Figure S1 of the Supporting Information. Superposition of the minor conformers also reveals their structural similarity, as shown in Figure S2 of the Supporting Information. Only those atoms pertaining to the macrocycle in each case were aligned, minimizing the root-mean-square differences. RMSD values of 0.99 and 1.19 Å, respectively, were obtained between *trans*DDB*cis* **1**(a) and *trans*DDB*trans* **1**(b) on one hand and between *cis*DDB*cis* **1**(c) and *cis*DDB*trans* **1**(d) on the other.

These molecular dynamics simulations were not implemented with a view to predicting the experimentally observed conformational isomer ratios of aplidine in DMSO. On the contrary the approach we describe here is a combined one in which the proportions and configurations of the different *cis*/*trans*-isomers have been determined by NMR experiments. The computer simulations are used only to model the conformational preferences of each of these isomers in turn and NMR data, in particular the NOE-derived interatomic distances, are used as to validate these simulations.

Conclusions

The origin of the observed conformational isomerism in aplidine is slow rotation about the Leu^7-Pro^8 and Pro^8-Pyr tertiary amide bonds. This conformational equilibrium, which leads to the generation of four distinct isomers present in a ratio of 47:33:13:7 is summarized graphically in Scheme 1.

It is noteworthy that the conformation of the macrocycle in all four isomers is essentially unchanged with respect to that of didemnin B and that variation in the overall three-dimensional structures is a consequence only of the disposition of the molecule's side-chain. More specifically, the overall three-dimensional structures of the major isomers *trans*DDB*cis* **1**(a) and *trans*DDB*trans* **1**(b) are broadly similar and both are similar to the structure reported for didemnin B. The predominance of these isomers in the mixture is accounted for by each isomer being stabilized by a hydrogen bond between the Thr^6 amino group and a different carbonyl group of the terminal pyruvyl unit. The minor isomers *cis*DDB*cis* **1**(c) and *cis*DDB*trans* **1**(d), which account for up to 20% of the global population have extended side chains, which do not form hydrogen bonds to the macrocycle. Their overall three-dimensional structures are also broadly similar.

It is clear that aplidine can access a range of conformations in solution. Such plasticity suggests that the molecule may have a range of different conformational ensembles available to it depending on its environment. It seems reasonable to suggest that, as we have observed in going from $CDCl_3$ to DMSO, in the various environments that aplidine might encounter in vivo, the range

SCHEME 1. Conformational Equilibrium in Aplidine in DMSO

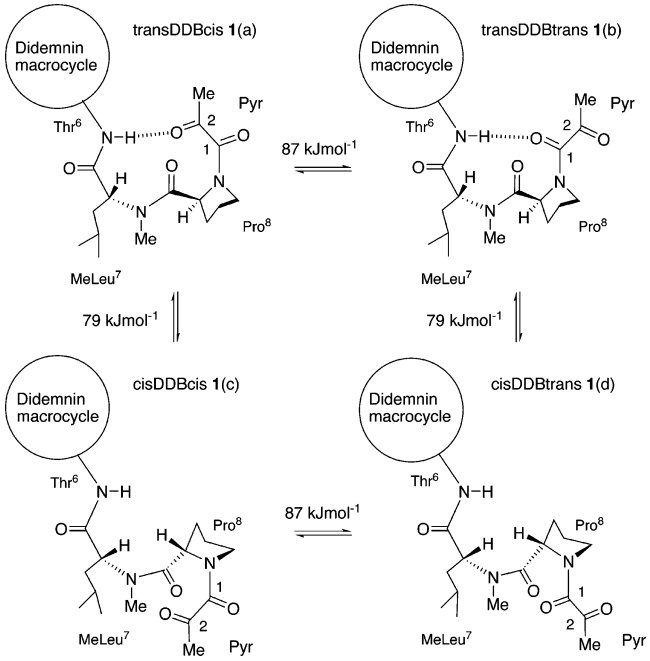

of populated conformations might be different. It might well be that the conformation necessary for its biological activity is present only as a minority within these ensembles.

Our results show that three-dimensional structures in which the molecule's side-chain does not adopt β-turn-type conformations are available to aplidine and account for up to 20% of the total population in DMSO. This is the first time that such extended side-chains have been unambiguously observed in the didemnins and the possibility that extended side-chain conformations play an important role in the biological activity of aplidine, the most active didemnin known to date, cannot be ruled out. This lends support to the notion that the adoption of a β-turn type conformation in the didemnin's side-chain is not a prerequisite for biological activity.

Experimental Section

Nuclear Magnetic Resonance Spectroscopy. A 15 mM degassed solution of synthetic[19] DDB in DMSO-d_6 (>99.98% deuterium incorporation) was used for all NMR experiments described in this study. 2D-*soft*-F1-NOESY and 2D-*soft*-F1-TOCSY spectra were registered at 298K on a Bruker-500 DMX Advance spectrometer equipped with a programmable pulse modulator in the proton channel, a gradient accessory and a $^1H\{^{13}C, ^{15}N\}$ triple resonance probe. All spectra were referenced using the residual resonance of DMSO at 2.49 ppm.

The 2D-*soft*-F1-TOCSY experiment with selective excitation of the amide region used a mixing time of 70 ms. Data along F1 were acquired in phase using the States-TPPI method.[32] The spectral window used was 4496 Hz in F2 and 1000 Hz in F1 and 128 increments and 64 accumulations were carried out. A final matrix of 2048 × 256 in F2 and F1, respectively, was obtained after zero-filling. The spectra were not symmetrized.

The 2D-*soft*-F1-TOCSY experiments with selective excitation of the α-carbon region used a mixing time of 70 ms. Data along F1 were acquired in phase using the States-TPPI

(32) Marion, D.; Ikura, M.; Tschudin, R.; Bax, A. *J. Magn. Reson.* **1989**, *85*, 393.

method. The spectral window used was 4496 Hz in F2 and 700 Hz in F1 and 128 increments and 64 accumulations were carried out. A final matrix of 2048 × 256 in F2 and F1, respectively, was obtained after zero-filling. The MLEV-17 method[33] was used to generate the spin-lock in the TOCSY experiment.

The 2D-*soft*-F1-NOESY experiments with selective excitation of the amide region used a mixing time of 300 ms. Data along F1 were acquired in phase using the States-TPPI method. The spectral window used was 4496 Hz in F2 and 1000 Hz in F1 and 256 increments and 64 accumulations were carried out. A final matrix of 2048 × 512 in F2 and F1, respectively, was obtained after zero-filling.

The 2D-*soft*-F1-NOESY experiments with selective excitation of the α-carbon region used a mixing time of 300 ms. Data along F1 were acquired in phase using the States-TPPI method. The spectral window used was 4496 Hz in F2 and 700 Hz in F1 and 256 increments and 64 accumulations were carried out. A final matrix of 2048 × 512 in F2 and F1, respectively, was obtained after zero-filling.

All nonselective proton 90° pulses were of 8 μs duration. The selective π pulses used to refocus the magnetization were RE-BURP pulses[34] of 5 ms duration, shifted 1600 Hz with respect to the carrier frequency to excite the amide region and of 10 ms duration, shifted 250 Hz to excite the α-carbon region. These pulses were generated using the ShapePulse program of the Bruker NMR software. The strengths of the G1 and G2 gradients during the DPFGSE train were 25 and 17 Gcm^{-1} of 1 and 1.17 ms duration, respectively. A delay of 200 μs followed all gradients for eddy current recovery. All 2D spectra were transformed after multiplying the time-domain data with an unshifted Gaussian window function along both the F1 and F2 dimensions. NOE build-up curves were generated from five conventional NOESY experiments (mixing times 50 ms, 100 ms, 150, 200, and 300 ms) at 800 MHz using the distance between the β-H of Pro[8] for calibration purposes.

Molecular Mechanics/Dynamics Simulations. Molecular mechanics/dynamics calculations were performed on Silicon Graphics 02 (MIPS R5000 processor) and Octane (MIPS R12000 processor) computers running IRIX 6.5, using the CHARMM program package[35] (versions 29b1 and 24b2, respectively) and the well-established CHARMm 23.1 force field.[30,31] An initial structure of the *trans*-Pyr-Pro[8] isomer for modeling studies was produced by editing the reported X-ray crystal structure of didemnin B. Three-dimensional starting structures for each of the other conformational isomers were obtained by manipulating the relevant torsions angles, and each of these was subjected to computer simulation separately. Both the CHARMm all-atom and united-atom representations of the molecule were modeled, the latter having all polar hydrogens explicitly represented. Charges were assigned to the atoms using the method described by Gasteiger and Marsili[36] and their suitability was confirmed by comparison with ESP charges derived from AM1-optimized small substructures for pyruvyl prolines, dimethyltyrosine and *N*-methyl amides employing MOPAC6. The GAUSSIAN94 program package, using the Hartree−Fock 6-31G* basis set was used to check that the force field parametrization for the pyruvamide function was adequate. After energy minimization, each of the four initial structures served as the starting point for NVE molecular mechanics/dynamics calculations at 300K. These were performed without the introduction of restraints, incorporating both implicit (ϵ=1, 4.8, 45, and 80) and explicit solvent descriptions for H_2O and DMSO. For the latter cubic boxes of 30 Å side-length and 1000 TIP3P water molecules[37] and of 31 Å side-length and 216 DMSO molecules respectively,[38] applying periodic boundary conditions. After adequate heating and equilibration of the systems, evolution times were 10ns for the all-atom implicit solvent simulations, 40 ns for all united-atom implicit solvent simulations, 4 ns for the DMSO united-atom explicit solvent simulation and 2 ns for the united-atom H_2O explicit solvent simulation. Structures were saved periodically from each trajectory for further analyses. Trajectories were analyzed for bond distances, torsion angles, and hydrogen bonds by extracting the relevant information from the CHARMM output files.

Acknowledgment. We thank Dr. Michael Thormann, Morphochem AG, München, Germany, for useful discussions. This work was partially supported by PharmaMar, SA, Madrid, and by grants from MCYT-FEDER (BIO2002-2301) and Generalitat de Catalunya (Grup Consolidat 1999SGR0042 and Centre de Referència en Biotecnologia).

Supporting Information Available: Tables (21 in all) of ^1H and ^{13}C NMR chemical shifts, of bond distances obtained from NOE build-up curves and from molecular modeling, of torsion angles found in the implicit and explicit solvent modeling studies and of H-bonds found in implicit and explicit solvent modeling studies, for all four conformational isomers of aplidine. A graphic showing the superposition of representative snapshots from the explicit DMSO trajectories for *trans*-DDB*cis* **1**(a) and *trans*DDB*trans* **1**(b). Another showing the superposition of representative snapshots from the explicit DMSO trajectories for *cis*DDB*cis* **1**(c) and *cis*DDB*trans* **1**(d). A copy of the 500 MHz ^1H NMR spectrum of aplidine in DMSO-d_6 and a graphic showing the numbering scheme for DDB used in this work. This material is available free of charge via the Internet at http://pubs.acs.org.

JO034798R

(33) Bax, A.; Davis, D. G. *J. Magn. Reson.* **1985**, *65*, 355.
(34) Geen, H.; Freeman, R. *J. Magn. Reson.* **1991**, *93*, 93.
(35) Brooks, B. R.; Bruccoleri, R. E.; Olafson, B. D.; States, D. J.; Swaminathan, S.; Karplus, M. *J. Comput. Chem.* **1983**, *4*, 187.
(36) Gasteiger, J.; Marsili, M. *Tetrahedron* **1980**, *36*, 3219.
(37) Jorgensen, W. L.; Chandrasekhar, J.; Madura, J. D.; Impey, R. W.; Klein, M. L. *J. Chem. Phys.* **1983**, *79*, 926.
(38) Liu, H.; Mueller-Plathe, F.; van Gunsteren, W. F. *J. Am. Chem. Soc.* **1995**, *117*, 4363.